Hyperfine Interact
DOI 10.1007/s10751-012-0697-1

Possible cage motion of interstitial Fe in α-Al_2O_3

H. P. Gunnlaugsson · K. Johnston · H. Masenda · R. Mantovan · T. E. Mølholt · K. Bharuth-Ram · H. P. Gislason · G. Langouche · M. B. Madsen · D. Naidoo · S. Ólafsson · G. Weyer · the ISOLDE Collaboration

Abstract In addition to spectral components due to Fe^{2+} and Fe^{3+}, a single line is observed in emission Mössbauer spectra following low fluence ($<10^{15}$ cm^{-2}) implantation of ^{57}Fe*, ^{57}Mn and ^{57}Co in α-Al_2O_3. For the ^{57}Co and ^{57}Mn implantations, the intensity of the single line is found to depend on the emission angle relative to the crystal symmetry axis. This angular dependence can be explained by a non-isotropic f-factor and/or motion of the Fe ion between sites in an interstitial cage. It is argued

H. P. Gunnlaugsson (✉) · G. Weyer
Department of Physics and Astronomy, Aarhus University, 8000 Aarhus C, Denmark
e-mail: hpg@phys.au.dk

K. Johnston · the ISOLDE Collaboration
Physics Department, ISOLDE/CERN, 1211 Geneva 23, Switzerland

H. Masenda · D. Naidoo
School of Physics, University of the Witwatersrand, WITS 2050, South Africa

R. Mantovan
Laboratorio MDM, IMM-CNR, Via Olivetti 2, 20864 Agrate Brianza (MB), Italy

T. E. Mølholt · H. P. Gislason · S. Ólafsson
Science Institute, University of Iceland, Dunhaga 3, 107 Reykjavík, Iceland

K. Bharuth-Ram
School of Physics, University of KwaZulu-Natal, Durban 4001, South Africa

K. Bharuth-Ram
iThemba LABS, P.O. Box 722, Somerset West 7129, South Africa

G. Langouche
Instituut voor Kern- en Stralingsfysica, University of Leuven, 3001 Leuven, Belgium

M. B. Madsen
Niels Bohr Institute, University of Copenhagen, 2100 Copenhagen, Denmark

Published online: 07 November 2012

that interstitial cage motion is a more likely explanation, as this can account for the lack of quadrupole splitting of the line.

Keywords α-Al_2O_3 · Ion-implantation · ^{57}Mn · Emission Mössbauer spectroscopy

1 Introduction

Substitutional Fe^{3+} impurities in α-Al_2O_3 have been of interest since the 1960's since much of the theory behind slow paramagnetic relaxations in Mössbauer spectra was developed in studies of such impurities [1].

Emission ^{57}Fe Mössbauer spectra obtained after ion-implantation of $<10^{15}$ cm^{-2} ^{57}Co [2], ^{57}Mn [3, 4], and Coulomb excited ^{57}Fe* [5] contain spectral components characteristic of high-spin Fe^{2+}, Fe^{3+} and a single line with room temperature isomer shift of ∼0.54 mm/s of disputed origin. For implantations at $>10^{15}$ cm^{-2} this line is not observed in the spectra [6, 7].

Laubach et al. [5] suggested that the single line was due to Fe^{3+} showing fast spin relaxation attributed to the implantation process. The spectra presented by Laubach et al. do not show evidence of slowly relaxing Fe^{3+}. This might be because their spectra were only recorded in a narrow velocity range, and they might have missed the slowly relaxing Fe^{3+} with low intensity in the wings of the spectra. Another possibility is that slowly relaxing Fe^{3+} was less present in their samples because of physical reasons as e.g. their Fe concentration was at least an order of magnitude lower than in this ISOLDE work and their measurement time window an order of magnitude shorter.

Deszi et al. [2] observed simultaneously slow paramagnetic Fe^{3+}, broad lined Fe^{2+} and the single line, and favoured the conclusion that this line was due to a charge state in between Fe^{2+} and Fe^{3+} due to rapid electron hopping akin to what is observed for iron on octahedral sites in magnetite [8].

Kobayashi et al. [4] suggested that this line was due to Fe^{3+}. However, they presented only spectra in a narrow velocity range and their isomer shifts seem to have lower values than observed in other studies [2, 3, 5].

Gunnlaugsson et al. [3] noticed the absence of a quadrupole splitting of this line and in an initial interpretation suggested that it was due to Fe in nano-precipitates of cubic η-Al_2O_3.

In this contribution we present additional measurements of the angular dependence of spectra obtained from ^{57}Mn and ^{57}Co implanted samples, which further restrict the possible interpretation of the origin of this line.

2 Experimental

Two sets of emission Mössbauer Spectroscopy (MS) measurements were made on single crystal α-Al_2O_3 samples, implanted respectively with ^{57}Mn to a maximum concentration of 10^{-3} at. % and ^{57}Co/^{57}Fe to a maximum concentration of 0.18 at. %.

Clean beams of ^{57}Mn ($T_{1/2} = 1.5$ min.) are produced at the ISOLDE facility at CERN following 1.4 GeV proton induced fission in UC_2 target and elemental selective laser ionization [9] with fluence ∼10^8 ^{57}Mn/s. After acceleration to

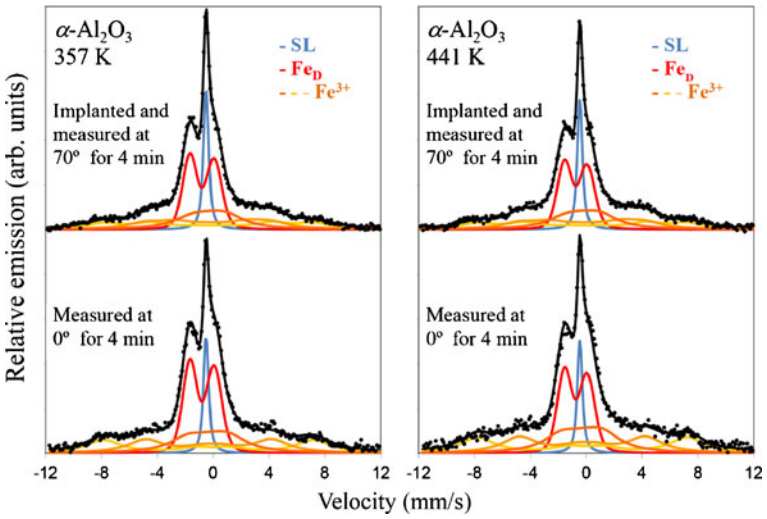

Fig. 1 ^{57}Fe emission spectra obtained after implantation of ^{57}Mn into α-Al_2O_3 single crystals held at the temperatures and emission angles indicated. The crystals were mounted on a magnet with external magnetic field $B_{ext} \sim 0.3$ T parallel to the *c*-axis of the crystals

40–50 keV, the beam was implanted into single crystal α-Al_2O_3 samples 20° relative to the sample normal and *c*-axis. Emission Mössbauer spectra were obtained using a resonance detector equipped with stainless-steel electrodes, mounted on a conventional drive system at 70° relative to the sample normal and 90° relative to the beam direction. Emission Mössbauer spectra measured under a 70° emission angle relative to the sample normal were obtained during the implantation for 4 min. Thereafter, the sample was rotated and spectra recorded under a 0° emission angle during the decay of ^{57}Mn for 4 min. This process was repeated several times to gather data with sufficient statistics. Possible annealing effects were studied with time-delayed measurements [10]. In all cases, samples were implanted with less than 5×10^{12} ^{57}Mn/cm^2.

Beams of ^{57}Co (and ^{57}Fe impurities) are produced at the ISOLDE facility at CERN following 1.4 GeV proton induced spallation in a YO target. Following acceleration to 50 keV, the beam was implanted into single crystal α-Al_2O_3 samples at ~0° relative to the sample normal and *c*-axis. The sample prepared received a fluence of 3×10^{12} ^{57}Co/cm^2 and 5×10^{14} ^{57}Fe/cm^2. Emission Mössbauer spectra were obtained under different emission angles by mounting the sample on a rotatable holder and by using the same stainless-steel resonance detector as used for the ^{57}Mn measurements mounted on a conventional drive system. Velocities and isomer shifts are given relative to the spectrum of α-Fe at room temperature.

3 Results

Figure 1 shows ^{57}Fe emission spectra obtained after implantation of ^{57}Mn into α-Al_2O_3 single crystals.

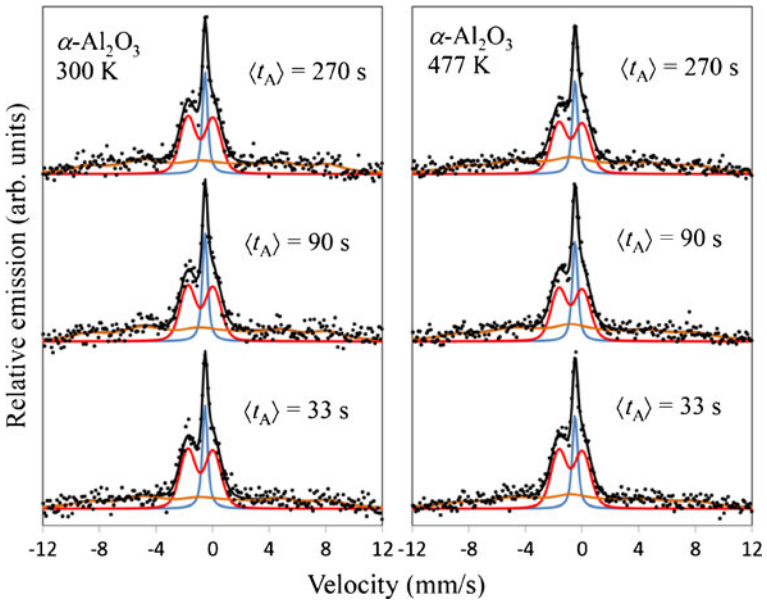

Fig. 2 Mössbauer spectra obtained from time-delayed measurements, following implantation of ^{57}Mn into α-Al_2O_3 single crystals at the temperatures indicated. Spectral components and average annealing times are indicated. The spectra were obtained under a 60° emission angle

The spectra have been analysed in terms of the same components that were used in [3]: An asymmetric quadrupole split component, Fe_D, assigned to Fe^{2+} in a damage environment, a single line, SL (the subject of this study) and Fe^{3+} showing slow paramagnetic relaxation, which was analysed in terms of three sextets assigned to three Kramers doublets with magnetic hyperfine splitting $B_{hf} \propto |S_Z|$ [11]. A small contribution from a component tentatively assigned to Fe^{4+} in ref. [3], dominating the central part of spectra at $T > 600$ K, has been omitted in the present analysis. The hyperfine parameters extracted from this analysis are in good agreement with those obtained in [3].

Visual inspection of the spectra in Fig. 1 shows clearly less intensity of the SL line in the spectra obtained under 0°. This could either be attributed to a real angular dependence of the intensity of the SL or to annealing effects, since the 0° measurements always took place after the 70° measurements. Annealing effects might be expected if the SL is due to Fe in an implantation induced damage environment that is unstable at the measurement/implantation temperatures on the timescale of our measurements (minutes). To test this hypothesis, spectra were obtained using time-delayed measurements [10] as shown in Fig. 2.

The main difference in the experimental conditions for the spectra shown in Figs. 1 and 2 is that the spectra in Fig. 2 were obtained without an external field and the Fe^{3+} component was consequently analysed in terms of an empirical model [3, 12]. At both temperatures, no significant decrease in the intensity of the SL component is evident. If the reduced intensity of the SL observed in the angular measurements (Fig. 1) were due to annealing effects, there should have been clear indications of such effects also

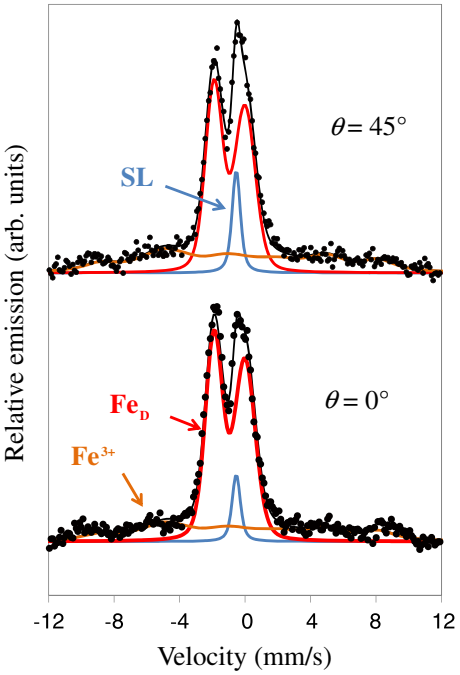

Fig. 3 Emission Mössbauer spectra obtained at room temperature from the ^{57}Co/^{57}Fe implanted sample

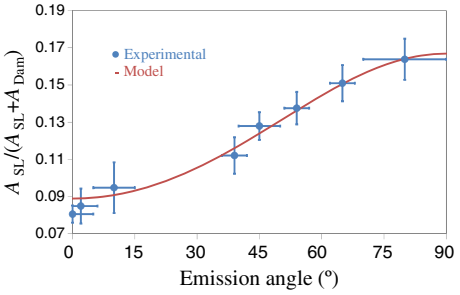

Fig. 4 Relative area of the SL as a function of emission angle

in Fig. 2. This result thus shows that the observed angular dependence of the intensity of the SL is not due to annealing effects.

To study the angular dependence in more detail, a sample implanted with ^{57}Co/^{57}Fe was measured at various emission angles at room temperature. Typical Mössbauer spectra are shown in Fig. 3.

In these measurements, the absolute area of the SL is not easily determined. This is partly due to the low activity of the sample. With the resonance detector only ~0.2 c/s are recorded, and instability during measurement can result in noise making the absolute area difficult to evaluate. From the ^{57}Mn measurement (cf. Figs. 1 and 2), it is known that the absolute area of Fe_D is independent of the emission angle, therefore the area ratio of the SL (A_{SL}) relative to the sum of the areas of Fe_D (A_{Dam}) and SL is determined better. This dependency is shown in Fig. 4.

4 Discussion

The angular dependence of the SL is incompatible with the interpretation of this component being due to Fe in cubic η-Al_2O_3 nano-precipitates [3] and alternative explanations have to be sought. At least two effects can result in an angular dependence of the intensity of the SL: an anisotropic f-factor and/or cage motion of interstitial Fe.

In the case of an anisotropic f-factor, the observed f-factor (proportional to the intensity of the line) can be written as [13]

$$f(\theta) = f_{\perp} \exp\left(-\varepsilon \cos^2 \theta\right). \tag{1}$$

Here $\varepsilon = -\ln\left(f_{||}/f_{\perp}\right)$, where $f_{||}$ and $f_{\perp}$ are the f-factors parallel to and perpendicular to the c-axis, respectively. Assuming that the f-factor of Fe_D is isotropic, the area ratio $A_{SL}/(A_{SL} + A_{Dam})$ (A_{Dam} is the area of Fe_D) will be proportional to the expression in (1). Analysis in terms of this model gives $\varepsilon = 0.6(1)$ or $f_{||}/f_{\perp} = 0.55(10)$; this is indicated by the solid line in Fig. 4.

Interstitial cage motion of Fe has been observed in, e.g., Al [14] and α-Zr [15]. Instead of the Fe atom occupying a well-defined interstitial site, it is found in specific equivalent locations around this site. The energy difference between such sites can be as low as a few tenths of meV, resulting in fast jumps between these sites at temperatures >50 K relative to the lifetime of the Mössbauer state. When the jump rate is fast compared to the lifetime of the Mössbauer state, the apparent intensity (I_r) can be evaluated according to [14]

$$I_r = \left| \frac{1}{Z} \sum_{j=1}^{Z} e^{i\mathbf{k}\cdot\mathbf{r}_j} \right|^2, \tag{2}$$

where the sum is taken over the Z jump possibilities, $\mathbf{k}$ is the wave-vector of the outgoing radiation and $\mathbf{r}_j$ the jump vectors.

The experimental data does not give any details on the jump mechanism. The simplest cage motion that can be imagined is a single jump along the c-axis. For that geometry, (2) becomes

$$I_r = \cos^2\left(\frac{Er}{\hbar c}\cos(\theta)\right), \tag{3}$$

where E is the transition energy (14.4 keV), r the jump length, $\hbar$ the reduced Planck's constant and c the speed of light. Assuming that the f-factor of Fe_D is isotropic, the area ratio $A_{SL}/(A_{SL} + A_{Dam})$ will be proportional to the expression in (3). Analysis in terms of this model gives $r = 0.10(2)$ Å, and a solid line in Fig. 4 which coincides with the line given by (1).

This is not necessarily the only type of cage motion that can explain the experimental data. It is possible to construct different types of cages ($Z > 2$) which can explain the experimental data, but if the simplest cage can fit the experimental data, more complex cages will undoubtedly do also.

In both models the Fe atoms responsible for the SL are assumed to occupy a non-regular lattice site and hence a quadrupole splitting is expected. However, if the interstitial cage motion takes the Fe atom to positions where the average of the quadrupole interaction cancels out on the measurement time scale [16], this

could offer an explanation for the lack of a quadrupole splitting. At this stage we cannot indicate a potential interstitial site with these properties within the lattice structure. It could possibly be associated with metastable vacancy defects, since it is not observed at elevated temperatures [3]. However, the important issue of this report is the documentation of the angular dependence of the SL and its possible origins.

The consistency of the ^{57}Co data (Fig. 4) can be checked with the results from the eMS measurements on the ^{57}Mn implanted α-Al_2O_3 samples (Figs. 1 and 2). Evaluation of the ratio of $A_{SL}/(A_{SL} + A_{Dam})$ obtained at the two emission angles in the ^{57}Co measurements gives (from Fig. 4)

$$\frac{\left(\frac{A_{SL}}{A_{SL}+A_{Dam}}\right)_{\theta=60^\circ}}{\left(\frac{A_{SL}}{A_{SL}+A_{Dam}}\right)_{\theta=0^\circ}} = 1.6\,(1)\,.$$

From ^{57}Mn data this ratio equals 1.4(1) at 357 K and 1.3(1) at 441 K (room temperature data do not exist), which seems to be in reasonable agreement.

Assuming a polycrystalline environment for Fe gives an average $A_{SL}/(A_{SL} + A_{Dam}) = 0.14(1)$ which is slightly lower than the values found by Dészi et al. [2] (0.17(1) and 0.23(1)). However, one should bear in mind that this value may depend on the total implantation fluence.

5 Conclusions

The intensity of the single line observed in emission Mössbauer spectra following low fluence ($<10^{15}$ cm^{-2}) implantation of ^{57}Fe* [5], ^{57}Mn [3, 4] and ^{57}Co [2] shows angular dependence. The angular dependence can be explained by a non-isotropic f-factor and/or interstitial cage motion of the Fe ion. The experimental data cannot determine which model is more appropriate, but the absence of a quadrupole splitting of the line points towards interstitial cage motion of the probe ion.

Acknowledgements This work was supported by the European Union Seventh Framework through ENSAR (contract no. 262010). R. Mantovan acknowledges support from MIUR through the FIRB Project RBAP115AYN "Oxides at the nanoscale: multifunctionality and applications". K. Bharuth-Ram, H. Masenda, and D. Naidoo acknowledge support from the South African National Research Foundation and the Department of Science and Technology. H. P. Gislason, S. Ólafsson and T. E. Mølholt acknowledges support from the Icelandic Research Fund. Financial support of the German BMBF Contract No. 05KK4TS1/9 is also gratefully acknowledged.

References

1. Wertheim, G.K., Remaika, J.P.: Mössbauer effect hyperfine structure of trivalent Fe^{57} in Corundum. Phys. Lett. **10**, 14–15 (1964)
2. Dézsi, I., Szucs, I., Fetzer, Cs., Pattyn, H., Langouche, G., Pfannes, H.D., Magalhães-Paniago, R.: Local interactions of ^{57}Fe after electron capture of ^{57}Co implanted in α-Al_2O_3 and in α-Fe_2O_3. J. Phys., Condens. Matter **12**, 2291–2296 (2000)
3. Gunnlaugsson, H.P., Mantovan, R., Mølholt, T.E., Naidoo, D., Johnston, K., Masenda, H., Bharuth-Ram, K., Langouche, G., Ólafsson, S., Sielemann, R., Weyer, G., Kobayashi, Y., ISOLDE Collaboration: Mössbauer spectroscopy of ^{57}Fe in α-Al_2O_3 following implantation of ^{57}Mn*. Hyperfine Interact. **198**, 5–14 (2010)

4. Kobayashi, Y., Nagatomo, T., Yamada, Y., Mihara, M., Sato, W., Miyazaki, J., Sato, S., Kitagawa, A., Kubo, M.K.: Anticoincidence measurement of ^{57}Fe Mössbauer spectra obtained after ^{57}Mn implantation: application to Fe in α-Al_2O_3. Hyperfine Interact. **198**, 173–178 (2010)
5. Laubach, S., Schwalbach, P., Hartick, M., Kankeleit, E., Keck B., Sielemann, R.: Implantation of Coulomb excited ^{57}Fe. Hyperfine Interact. **53**, 75–92 (1990)
6. Dézsi, I., Coussement, R., Feher, S., Langouche, G., Fetzer, Cs.: The charge states of iron in insulators implanted with ^{57}Co and ^{57}Fe. Hyperfine Interact. **29**, 1275–1278 (1986)
7. McHargue, C.J., Farlow, G.C., Sklad, P.S., White, C.W., Perez, A., Kornilios, N., Marest, G.: Iron ion implantation effects in Sapphire. Nucl. Instrum. Methods B **19/20**, 813–821 (1987)
8. Kündig, W., Hargrove, R.S.: Electron hopping in magnetite. Solid State Commun. **7**, 223–227 (1969)
9. Fedoseyev, V.N., Bätzner, K., Catherall, R., Evens, A.H.M., Forkel-Wirth, D., Jonsson, O.C., Kugler, E., Lettry, J., Mishin, V.I., Ravn, H.L., Weyer, G., the ISOLDE Collaboration: Chemically selective laser ion source of manganese. Nucl. Instrum. Methods B **126**, 88–91 (1997)
10. Gunnlaugsson, H.P., Weyer, G., Mantovan, R., Naidoo, D., Sielemann, R., Bharuth-Ram, K., Fanciulli, M., Johnston, K., Olafsson, S., Langouche, G.: UIsothermal defect annealing in semiconductors investigated by time-delayed Mössbauer spectroscopy: application to ZnO. Hyperfine Interact. **188**, 85–89 (2009)
11. Gunnlaugsson, H.P., Sielemann, R., Mølholt, T.E., Dlamini, W.B., Johnston, K., Mantovan, R., Masenda, H., Naidoo, D., Sibanda, W.N., Bharuth-Ram, K., Fanciulli, M., Gíslason, H.P., Langouche, G., Ólafsson, S., Weyer, G., the ISOLDE Collaboration: Magnetism in iron implanted oxides: a status report. Hyperfine Interact. **197**, 43–52 (2010)
12. Mølholt, T.E., Mantovan, R., Gunnlaugsson, H.P., Naidoo, D., Ólafsson, S., Bharuth-Ram, K., Fanciulli, M., Johnston, K., Kobayashi, Y., Langouche, G. Masenda, H., Sielemann, R., Weyer G., Gíslason, H.P.: Observation of spin-lattice relaxations of dilute Fe^{3+} in MgO by Mössbauer spectroscopy. Hyperfine Interact. **197**, 89–94 (2010)
13. Goldanskii, V.I., Makarov, E.F.: Fundamentals of gamma-resonance spectroscopy. In: Goldanskii, V.I., Herber, R.H. (eds.) Chemical Applications of Mössbauer Spectroscopy, pp. 1–113. Academic Press, New York (1968)
14. Petry, W., Vogl, G.: Mössbauer study of localized diffusion in an interstitial cage I. Model calculations. Z. Phys., B Condens. Matter **45**, 207–213 (1982)
15. Yoshida, Y., Menningen, M., Sielemann, R., Vogl, G., Weyer, G., Schröder, K.: Local atomic-jump process of iron in α-Zr. Phys. Rev. Lett. **61**, 195–198 (1988)
16. Tjon, J.A., Blume, M.: Mössbauer spectra in a fluctuating environment II. Randomly varying electric field gradients. Phys. Rev. **165**, 456–461 (1968)